Res Chem Intermed
DOI 10.1007/s11164-015-2246-4

Magnetic Fe_3O_4–BF_3: highly efficient Lewis acid catalyst for the synthesis of α-aminonitriles

Mohsen Shekouhy[1] · Ali Moaddeli[2] · Ali Khalafi-Nezhad[1]

Received: 27 April 2015 / Accepted: 25 August 2015

Abstract Fe_3O_4 magnetic nanoparticle-supported BF_3 was prepared as a new magnetically separable Lewis acid catalyst and successfully used for the one-pot synthesis of α-aminonitriles. A broad range of substrates including the aromatic and heteroaromatic aldehydes, cyclic ketones (cyclopentanone, cyclohexanone and cycloheptanone), aryl–alkyl ketones, diaryl ketones and tetralones, isatin derivatives and acenaphthenequinone were condensed with amines (aliphatic and aromatic) and trimethylsilyl cyanide. All reactions were completed in short times and products were obtained in good to excellent yields. The catalyst could be recycled and reused several times without any loss of efficiency. Finally, α-aminonitrile containing adenine was successfully synthesized.

Keywords α-Aminonitrile · Fe_3O_4–BF_3 magnetic nanoparticle · Diversity-oriented synthesis · Magnetically separable catalyst · Lewis acid catalysis

Introduction

The main focus of catalysis research in the past decade has been to enhance catalytic activity and selectivity and there has not been not any serious attention given to catalyst recovery. In spite of the fact that homogeneous catalysts are well defined on a molecular level and are readily soluble in reaction mediums and such single-site catalysts are highly accessible to the substrates with high catalytic activity and selectivity, removing then from reaction mixtures to avoid contamination of the product requires expensive and tedious purification steps [1–4]. So, recycling of

✉ Ali Khalafi-Nezhad
khalafi@chem.susc.ac.ir

[1] Department of Chemistry, College of Sciences, Shiraz University, Shiraz 71454, Iran

[2] Department of Chemistry, Yazd University, Yazd 89195-741, Iran

Published online: 10 September 2015

homogeneous catalysts is an important issue in the sustainable and large-scale production of fine chemicals. Liquid–liquid and solid–liquid separation are two major methods for the separation of catalysts form reaction media. Solid–liquid techniques are based on the immobilization of species with catalytic activity on solid supports containing organic polymers or resins and inorganic oxide. In the case of solid particles suspended in a liquid, the rate of transfer of reactants within the liquid to the catalyst is inversely proportional to the particle diameter. Thus, the activity (and the selectivity) of the suspended catalyst will benefit from decreasing the particle size [5]. It is worth mentioning at this point that the dispersion of most conventional heterogeneous catalysts in liquid media is poor and, in most cases, distinct solid–liquid separation occurs even after vigorous stirring. One way to overcome this drawback is to keep the size of the particles as small as possible [6–13]. However, particles with diameters of less than 100 nm are difficult to separate by filtration techniques and, in such cases, expensive ultracentrifugation is often the only way to separate product and catalyst. One important way to overcome this mistake is the application of magnetic nanoparticles (MNPs) as heterogeneous support, which can be easily removed from the reaction mixture by magnetic separation [14–18].

It is well known that boron compounds are very potent Lewis acids due to the electron deficiency of the boron core. There are many reports about the application of various catalytic systems based on boron compounds [19].

Between them, BF_3 is a potent and common material with a high-level Lewis acid property that is used as a Lewis acid catalyst in isomerization, alkylation, esterification, condensation, Mukaiyama aldol addition, and many other reactions [20]. Though BF_3 is a strong catalyst in many organic transformations, it is not a recoverable material and its application produces hazardous toxic waste. So, introducing of some appropriate methods to make this material a separable catalytic system is of great interest in Lewis acid-catalyzed organic synthesis. One useful way to attain this goal is connection of BF_3 on a heterogeneous support.

The addition of a cyanide anion to imines (the Strecker reaction) [21] provides one of the most important and straightforward methods for the synthesis of α-aminonitriles, which are useful intermediates for the synthesis of amino acids [22, 23] and nitrogen-containing heterocycles [24, 25], and other biologically useful molecules such as saframycin A, or phthalascidi [26]. Several modifications of the Strecker reaction have been reported, using a variety of cyanide reagents, such as alkaline cyanides [21, 27, 28], diethylphosphoro cyanidate [29], Bu_3SnCN [30] and Et_2AlCN [31], as well as catalysts such as $InCl_3$ [32], $BiCl_3$ [33], montmorillonite KSF clay [34], silica-based scandium(III) [35], SO_4^{2-}/ZrO_2 [36], ferric perchlorate [37], $Fe(Cp)_2PF_6$ [38], InI_3 [39], I_2 [40], $K_5CoW_{12}O_{40}.3WATER$ [41], vanadyl triflate [42], Fe_3O_4 [43], guanidine hydrochloride [44], xanthan sulfuric acid [45], $[Bmim]BF_4$ [46], silica sulfuric acid [47], hydrophobic sulfonic acid based nanoreactors [48] and silica-bonded S-sulfonic acid [49] under various reaction conditions. However, many of these methods suffer from some drawbacks such as the use of stoichiometric reagents and hazardous and often expensive catalysts, low yields of products, harsh reaction conditions, extended reaction times, tedious catalyst preparation procedures, the use of volatile and hazardous organic solvents,

non-compliance with "green" chemistry protocols and also require tedious workup leading to the generation of a large amount of toxic waste. Furthermore, many of these catalysts are deactivated or sometimes decomposed by amines and water that exist during imine formation. Also, it has been shown that trimethylsilyl cyanide (TMSCN) is a very effective, relatively safe and easy-to-handle cyanide source for this purpose [50–57]. Consequently, development of a general, efficient, inexpensive and environmentally benign method for the synthesis of α-aminonitriles is still in demand.

As a part of our continuing studies in developing efficient heterogeneous catalysts [58–60], we found that synthesis of α-aminonitriles via a one-pot three-component reaction can be efficiently achieved in the presence of Fe_3O_4 magnetic nanoparticles supported-boron trifluoride (BF_3–Fe_3O_4 MNPs) as a new magnetically separable heterogeneous Lewis acid catalyst in ethanol under ultrasonic irradiation at room temperature.

Experimental

Apparatus and analysis

Reagents and solvents were purchased from Merck, Fluka or Aldrich. Melting points were determined in capillary tubes in an electro-thermal C14250 apparatus. The progress of the reaction and the purity of compounds were monitored by thin layer chromatography (TLC) analytical silica gel plates (Merck 60 F250). All known compounds were identified by comparison of their melting points and proton nuclear magnetic resonance (^{1}H NMR) data with those in the authentic samples. The ^{1}H NMR (250 MHz) and Carbon 13 NMR (^{13}C NMR, 62.5 MHz) were run on a Bruker Avance DPX-250, Fourier transform (FT)-NMR spectrometer. Chemical shifts are given as δ values against tetramethylsilane (TMS) as the internal standard and J values are given in Hz. The elemental analysis was performed on a Perkin-Elmer 240-B microanalyzer. The ultrasound apparatus was a cleaning bath Wiseclear 770 W (Seoul, Korea). The operating frequency was 40 kHz and the output power was 200 W, estimated calorimetrically. The reaction flasks were located in the maximum energy area in the water bath, where the surface of the reactants (reaction vessel) is slightly lower than the level of the water, and the addition or removal of water controlled the temperature of the water bath. The temperature of the water bath was controlled at 25–30 °C. Moreover, the temperature of the reaction flask was monitored with an internal thermometer and it was stable between 36 and 40 °C during the progress of all reactions. All experiments performed in this work were repeated three times. The yield reported represents the average of the values obtained for each reaction. The X-ray diffraction (XRD) patterns were recorded on a Bruker D8 ADVANCE X-ray diffractometer using nickel-filtered Cu Kα radiation ($\lambda = 1.5406$ Å). Scanning electron micrograms were obtained using a KYKY-EM3200 instrument. Potentiometric data was collected using a pH/mV meter, AZ model 86502-pH/ORP. The inductively coupled plasma (ICP) analysis was determined using an ICP analyzer (Varian, Vista-Pro). F_3O_4 magnetic

nanoparticles were synthesized using a reported method [61]. The fluoride content of catalysts was determined based on a reported method [62].

Synthesis of 4-(3-bromopropoxy)benzaldehyde (9)

A mixture of *p*-hydroxybenzaldehyde (0.02 mol, 2.44 g), 1,3-dibromopropane (0.06 mol), K_2CO_3 (2.76 g, 0.02 mol) and tetrabutyl ammonium bromide (TBAB, 0.1 g) in acetonitrile (50 mL) was refluxed in a double-necked round-bottom flask (100 mL) equipped with a condenser for 10 h. After this time, the reaction mixture was cooled and the solvent was evaporated under reduced pressure and the resulting foam was dissolved in chloroform (150 mL) and washed with water (3 × 150 mL). The organic layer was dried over anhydrous Na_2SO_4 and evaporated. The crude product was purified by column chromatography on silica gel [eluting with a mixture of *n*-hexane and ethyl acetate (1:2), Rf = 0.6], giving the desired product as a white solid in 80 % yield (3.9 g).

Synthesis of 4-(3-(1,3-dimethyl-2,6-dioxo-1,2,3,6-tetrahydro-7*H*-purin-7-yl)-propoxy)benzaldehyde (1b)

To a double-necked 250-mL round-bottom flask equipped with a condenser containing an appropriate amount of presilylated adenine (0.01 mol, 2.79 g) and 4-(3-bromopropoxy)benzaldehyde (**9**) (0.01 mol, 2.41 g) diluted in freshly distilled, anhydrous tetrahydrofurane (100 mL), anhydrous tetrabutyl ammonium fluoride (TBAF, 2.62 g, 0.01 mol) in dried tetrahydrofurane (20 mL) was gradually added over 20 min. (For the production of presilylated adenine, please see Ref. [63]). Then, the mixture was heated at reflux temperature and the progress of the reaction was monitored by TLC. After reaction completion, the solvent was evaporated at reduced pressure and the residue was dissolved in chloroform (200 mL) and washed with water (3–100 mL). The organic layer was dried over Na_2SO_4 and concentrated to afford the crude product. The crude product was purified by column chromatography on silica gel [eluting with a mixture of *n*-hexane and ethyl acetate (1:2), Rf = 0.6], giving the desired product as a white solid in 78 % yield (2.31 g).

General procedure for the synthesis of α-aminonitriles

Aldehyde or ketone (1 mmol) and amine (1.2 mmol) were added to a mixture of Fe_3O_4–BF_3 (50 mg) and ethanol (5 mL) in a 25-mL Pyrex flask and the resulting mixture was continuously irradiated for 2 min. TMSCN (1.2 mmol) was added and the resulting mixture was continuously irradiated for the appropriate time (Table 2) at room temperature. The reactions were followed by TLC using *n*-hexane/ethyl acetate (3:1) as an eluent. The ultrasonic apparatus used, showed the temperature automatically so the temperature was controlled and fixed at room temperature by pouring cold water in the bath in the case of any elevation of temperature. After completion of the reaction, heterogeneous magnetic particles of the catalyst were separated with a magnet, washed with ethanol (5 mL), dried under reduced pressure for 24 h at 100 °C and kept for the next use. After catalyst isolation, water (20 mL)

was added and stirred magnetically for 5 min. Insoluble crude products were filtered and recrystallized from ethanol/water (4:1). In the case of oil products, appropriate amounts of ethyl acetate (5 mL, two times) were added; the organic layer was washed with brine (5 mL), dried ($MgSO_4$), and concentrated. The residue was chromatographed over silica gel (15-% ethyl acetate in hexane) to give a pure product.

Selected spectral data

2-(Butylamino)-2-(pyridin-3-yl)acetonitrile (Compound 4aw)

Colorless oil [65], υ_{max} (KBr): 3345, 3025, 2962, 2220 cm^{-1}. ^1H NMR [250 MHz, deuterated chloroform ($CDCl_3$)]: δ (ppm) 0.91 (t, $J = 7.9$ Hz, 3H), 1.20–1.38 (m, 2H), 1.46–1.60 (m, 2H), 3.08 (q, $J = 7.5$ Hz, 2H), 3.91–4.22 (m, 2H), 7.45 (d, $J = 8.0$ Hz, 1H), 7.83 (dd, $J = 2.0$, 8.0 Hz, 1H), 8.54 (d, $J = 8.5$ Hz, 1H), 8.85 (s, 1H). ^{13}C NMR (62.5 MHz, $CDCl_3$): δ (ppm) 13.9, 20.1, 32.3, 45.8, 49.0, 116.9, 123.0, 132.4, 134.0, 147.5, 150.3. Anal. Calcd for $C_{11}H_{15}N_3$: C, 69.81; H, 7.99; N, 22.20 %; found: C, 69.88; H, 7.81; N, 22.12 %.

2-(Phenylamino)hexanenitrile (Compound 4az)

White crystalline solid, mp: 58–59 °C (55–57 °C) [25] υ_{max} (KBr): 3352, 3015, 2945, 2230 cm^{-1}. ^1H NMR (250 MHz, $CDCl_3$): δ (ppm) 0.95 (t, $J = 7.5$ Hz, 3H), 1.20–1.48 (m, 2H), 1.55–1.67 (m, 2H), 3.10 (q, $J = 7.5$ Hz, 2H), 3.95–4.25 (m, 2H), 6.92–7.29 (m, 5H). ^{13}C NMR (62.5 MHz, $CDCl_3$): δ (ppm) 14.2, 22.1, 25.4, 31.5, 48.7, 113.0, 116.1, 117.6, 129.2, 147.9. Anal. Calcd for $C_{12}H_{16}N_2$: C, 76.55; H, 8.57; N, 14.88 %; found: C, 76.54; H, 8.50; N, 14.83 %.

2-(Benzylamino)-3-methylbutanenitrile (Compound 4ba)

Colorless oil (colorless oil) [25], υ_{max} (KBr): 3355, 3015, 2952, 2220 cm^{-1}. ^1H NMR (250 MHz, $CDCl_3$): δ (ppm) 1.03 (d, $J = 7.5$ Hz, 3H), 1.08 (d, $J = 7.5$ Hz, 3H), 1.52 (brs, 1H), 1.93 (m, 1H), 2.05–2.16 (distorted AB System, 2H), 3.27 (d, $J = 7.5$ Hz, 1H), 3.85 (d, $J = 12.8$ Hz, 1H,), 4.11 (d, $J = 12.8$ Hz, 1H), 7.24–7.44 (m, 5H). ^{13}C NMR (62.5 MHz, $CDCl_3$): δ (ppm) 18.2, 19.6, 31.7, 51.5, 56.5, 119.0, 127.1, 128.2, 128.9, 138.8. Anal. Calcd for $C_{12}H_{16}N_2$: C, 76.55; H, 8.57; N, 14.88 %; Found: C, 76.45; H, 8.51; N, 14.72 %.

1-(Phenylamino)cyclopentanecarbonitrile (Compound 4be)

White crystalline solid, mp: 54–57 °C (55–56) [65], υ_{max} (KBr): 3348, 3025, 2950, 2230 cm^{-1}. ^1H NMR (250 MHz, $CDCl_3$): δ (ppm) 1.40 (m, 2H), 1.55 (m, 2H), 1.88 (m, 2H), 2.12 (m, 2H), 3.98 (brs, 1H), 6.68 (d, $J = 7.5$ Hz, 2H,), 6.95 (t, $J = 7.5$ Hz, 1H), 7.18 (t, $J = 7.5$ Hz, 2H). ^{13}C NMR (62.5 MHz, $CDCl_3$): δ (ppm) 22.8, 33.9, 53.0, 113.8, 117.2, 119.8, 131.2, 143.8. Anal. Calcd for $C_{12}H_{14}N_2$: C, 77.38; H, 7.58; N, 15.04 %; Found: C, 77.25; H, 7.55; N, 14.99 %.

1-(p-Tolylamino)cyclopentanecarbonitrile (Compound 4bf)

White crystalline solid, mp: 55–57 °C (57–59) [65], υ_{max} (KBr): 3352, 3020, 2935, 2230 cm^{-1}. ^1H NMR (250 MHz, $CDCl_3$): δ (ppm) 1.45 (m, 2H), 1.55 (m, 2H), 1.87 (m, 2H), 2.10 (m, 2H), 2.31 (s, 3H), 3.97 (brs, 1H), 6.88 (d, $J = 7.8$ Hz, 2H,), 6.96 (d, $J = 7.8$ Hz, 2H). ^{13}C NMR (62.5 MHz, $CDCl_3$): δ (ppm) 22.5, 24.2, 32.7, 51.4, 113.0, 119.5, 126.4, 128.8, 143.5. Anal. Calcd for $C_{13}H_{16}N_2$: C, 77.96; H, 8.05; N, 13.99 %; Found: C, 77.90; H, 8.06; N, 13.92 %.

1-(Phenylamino)cycloheptanecarbonitrile (Compound 4bg)

White crystalline solid, mp: 55–57 °C (56–57) [65], υ_{max} (KBr): 3350, 3030, 2925, 2220 cm^{-1}. ^1H NMR (250 MHz, $CDCl_3$): δ (ppm) 1.25 (brs, 4H), 1.36 (brs, 4H), 1.70 (brs, 4H), 4.05 (s, 1H), 6.65 (d, $J = 8.0$ Hz, 2H), 6.85 (t, $J = 8.0$ Hz, 1H,), 7.05 (t, $J = 8.0$ Hz, 2H). ^{13}C NMR (62.5 MHz, $CDCl_3$): δ (ppm) 21.1, 27.9, 33.5, 52.0, 113.5, 117.7, 119.0, 127.5, 143.5. Anal. Calcd for $C_{14}H_{18}N_2$: C, 78.46; H, 8.47; N, 13.07 %; Found: C, 78.33; H, 8.41; N, 13.12 %.

1-(4-Bromophenylamino)cycloheptanecarbonitrile (Compound 4bh)

White crystalline solid, mp: 60–63 °C (62–64) [65], υ_{max} (KBr): 3405, 3025, 2930, 2230 cm^{-1}. ^1H NMR (250 MHz, $CDCl_3$): δ (ppm) 1.21 (brs, 4H), 1.35 (brs, 4H), 1.73 (brs, 4H), 4.02 (s, 1H), 6.87 (d, $J = 8.0$ Hz, 2H), 6.98 (d, $J = 8.0$ Hz, 2H,). ^{13}C NMR (62.5 MHz, $CDCl_3$): δ (ppm) 21.0, 27.6, 33.2, 51.8, 113.2, 115.4, 120.1, 133.8, 143.9. Anal. Calcd for $C_{14}H_{17}BrN_2$: C, 57.35; H, 5.84; N, 9.55 %; Found: C, 57.32; H, 5.72; N, 9.62 %.

2-Phenyl-2-(phenylamino)propanenitrile (Compound 4bi)

White crystalline solid, mp: 142–144 °C (143–145) [65], υ_{max} (KBr): 3320, 3046, 2225 cm^{-1}. ^1H NMR (250 MHz, $CDCl_3$): δ (ppm) 1.95 (s, 3H), 4.52 (brs, 1H), 6.75–6.88 (m, 3H), 7.25–7.38 (m, 5H), 7.40 (d, $J = 8.5$ Hz, 2H). ^{13}C NMR (62.5 MHz, $CDCl_3$): δ (ppm) 22.8, 66.5, 113.9, 120.1, 120.9, 127.6, 128.1, 128.8, 129.0, 130.1, 147.8. Anal. Calcd for $C_{15}H_{14}N_2$: C, 81.05; H, 6.35; N, 12.60 %; Found: C, 80.91; H, 6.33; N, 12.72 %.

2-(4-Bromophenylamino)-2-p-tolylpropanenitrile (Compound 4bj)

White crystalline solid, mp: 180–182 °C (179–181) [65], υ_{max} (KBr): 3338, 3075, 2950, 2308 cm^{-1}. ^1H NMR (250 MHz, $CDCl_3$): δ (ppm) 1.94 (s, 3H), 2.35 (s, 3H), 4.29 (brs, 1H), 6.65 (d, $J = 8.5$ Hz, 2H), 7.18 (d, $J = 8.5$ Hz, 2H), 7.25–7.39 (m, 4H). ^{13}C NMR (62.5 MHz, $CDCl_3$): δ (ppm) 21.8, 23.5, 68.4, 114.2, 115.8, 120.0, 127.0, 128.2, 128.7, 132.3, 137.7, 146.9. Anal. Calcd for $C_{16}H_{15}BrN_2$: C, 60.97; H, 4.80; N, 8.89 %; Found: C, 61.02; H, 4.88; N, 8.95 %.

2-(Isopropylamino)-2-(3-nitrophenyl)propanenitrile (Compound 4bk)

Yellow crystalline solid, mp: 118–119 °C (115–117) [65], υ_{max} (KBr): 3360, 3050, 2950, 2228 cm^{-1}. ^1H NMR (250 MHz, $CDCl_3$): δ (ppm) 1.05 (d, $J = 7.8$ Hz, 6H), 1.72 (brs, 1H), 1.91 (s, 3H), 2.80 (m, 1H), 7.69–7.75 (m, 2H), 8.09 (d, $J = 8.5$ Hz, 1H), 8.23 (d, $J = 2.0$ Hz, 1H). ^{13}C NMR (62.5 MHz, $CDCl_3$): δ (ppm) 23.4, 24.8, 46.0, 63.1, 119.5, 123.5, 62.5.0, 127.6, 131.8, 134.5, 147.0. Anal. Calcd for $C_{12}H_{15}N_3O_2$: C, 61.79; H, 6.48; N, 18.01 %; Found: C, 61.88; H, 6.45; N, 17.89 %.

2-(Benzylamino)-2,2-diphenylacetonitrile (Compound 4bk)

White crystalline solid, mp: 155–158 °C (155–157) [65], υ_{max} (KBr): 3355, 3060, 2225 cm^{-1}. ^1H NMR (250 MHz, $CDCl_3$): δ (ppm) 2.00–2.09 (distorted AB System, 2H), 1.90 (s, 1H), 7.23–7.35 (m, 15H). ^{13}C NMR (62.5 MHz, $CDCl_3$): δ (ppm) 46.6, 68.5, 114.0, 126.9, 127.5, 127.9, 128.0, 128.5, 129.2, 140.9, 143.6. Anal. Calcd for $C_{21}H1_8N_2$: C, 84.53; H, 6.08; N, 9.39 %; Found: C, 84.56; H, 6.17; N, 9.32 %.

2-(4-Bromophenylamino)-2,2-diphenylacetonitrile (Compound 4bm)

White crystalline solid, mp: 173–175 °C (171–173) [65], υ_{max} (KBr): 3360, 3045, 2230 cm^{-1}. ^1H NMR (250 MHz, $CDCl_3$): δ (ppm) 4.60 (brs, 1H), 6.50 (d, $J = 8.5$ Hz, 2H), 7.19 (d, $J = 8.5$ Hz, 2H), 7.21–7.35 (m, 10H). ^{13}C NMR (62.5 MHz, $CDCl_3$): δ (ppm) 68.5, 114.0, 114.6, 115.8, 126.2, 128.0, 129.5, 132.7, 143.5, 147.2. Anal. Calcd for $C_{20}H_{15}BrN_2$: C, 66.13; H, 4.16; N, 7.71 %; Found: C, 66.19; H, 4.23; N, 7.83 %.

3-Oxo-3-phenyl-2-(phenylamino)propanenitrile (Compound 4bn)

White crystalline solid, mp: 62–64 °C (59–61) [65], υ_{max} (KBr): 3460, 3010, 2950, 2230, 1695 cm^{-1}. ^1H NMR (250 MHz, $CDCl_3$): δ (ppm) 4.20 (brs, 1H), 5.05 (s, 1), 6.40 (d, $J = 8.0$ Hz, 2H), 6.63 (t, $J = 8.0$ Hz, 1H), 7.05 (t, $J = 8.0$ Hz, 2H), 7.45 (t, $J = 7.5$ Hz, 2H), 7.68 (t, $J = 7.7$ Hz, 1H), 7.81 (d, $J = 7.5$ Hz, 2H). ^{13}C NMR (62.5 MHz, $CDCl_3$): δ (ppm) 63.0, 113.0, 116.7, 126.5, 126.9, 128.0, 129.9, 133.2, 135.0, 143.8, 197.3. Anal. Calcd for $C_{15}H_{12}N_2O$: C, 76.25; H, 5.12; N, 11.86 %; Found: C, 76.20; H, 5.02; N, 11.94 %.

2-(p-Tolylamino)-3-oxo-3-phenylpropanenitrile (Compound 4bo)

White crystalline solid, mp: 65–68 °C (63–65) [65], υ_{max} (KBr): 3405, 3020, 2938, 2230, 1690 cm^{-1}. ^1H NMR (250 MHz, $CDCl_3$): δ (ppm) 1.95 (s, 3H), 4.00 (brs, 1H), 5.19 (s, 1), 6.50 (d, $J = 8.5$ Hz, 2H), 7.08 (d, $J = 8.5$ Hz, 2H), 7.44 (t, $J = 8.0$ Hz, 2H), 7.62 (t, $J = 8.0$ Hz, 2H), 7.88 (d, $J = 8.0$ Hz, 2H). ^{13}C NMR (62.5 MHz, $CDCl_3$): δ (ppm) 24.5, 62.5, 113.4, 116.0, 126.90, 126.98, 128.0, 129.1, 133.0, 135.5, 143.4, 197.0. Anal. Calcd for $C_{16}H_{14}N_2O$: C, 76.78; H, 5.64; N, 11.19 %; Found: C, 76.62; H, 5.71; N, 11.01 %.

1,2,3,4-Tetrahydro-1-(phenylamino)naphthalene-1-carbonitrile (Compound 4 bp)

White crystalline solid, mp: 120–121 °C (123–62.5) [65], υ_{max} (KBr): 3360, 3045, 2940, 2230 cm^{-1}. ^1H NMR (250 MHz, $CDCl_3$): δ (ppm) 1.55–1.70 (m, 2H), 2.08–2.23 (m, 2H), 2.88–2.95 (m, 2H), 4.60 (brs, 1H), 6.80–6.89 (m, 7H), 7.20 (t, J = 8.0 Hz, 2H). ^{13}C NMR (62.5 MHz, $CDCl_3$): δ (ppm) 14.8, 29.5, 38.5, 63.0, 113.0, 120.9, 121.0, 62.5.5, 127.3, 129.9, 134.0, 135.7, 147.0. Anal. Calcd for $C_{17}H_{16}N_2$: C, 82.22; H, 6.49; N, 11.28 %; Found: C, 82.12; H, 6.40; N, 11.33 %.

2-Oxo-3-(phenylamino)indoline-3-carbonitrile (Compound 7aa)

White crystalline solid, mp: 94–95 °C (91–92) [65], υ_{max} (KBr): 3390, 3300, 3040, 2960, 2235, 1668 cm^{-1}. ^1H NMR (250 MHz, $CDCl_3$): δ (ppm) 4.88 (brs, 1H), 6.85 (d, $J = 7.5$ Hz, 1H), 7.32–7.68 (m, 8H), 8.30 (s, 1H). ^{13}C NMR (62.5 MHz, $CDCl_3$): δ (ppm) 71.0, 111.3, 119.8, 121.0, 62.5.3, 126.7, 129.0, 131.3, 132.8, 140.5, 148.9, 152.9, 171.0. Anal. Calcd for $C_{15}H_{11}N_3O$: C, 72.28; H, 4.45; N, 16.86 %; Found: C, 72.10; H, 4.52; N, 16.95 %.

3-(p-Tolylamino)-2-oxoindoline-3-carbonitrile (Compound 7ab)

White crystalline solid, mp: 103–105 °C (99–101) [65], υ_{max} (KBr): 3400, 3298, 3035, 2960, 2230, 1670 cm^{-1}. ^1H NMR (250 MHz, $CDCl_3$): δ (ppm) 2.15 (s, 3H), 4.95 (brs, 1H), 6.98 (d, $J = 7.5$ Hz, 1H), 7.28–7.51 (m, 7H), 8.68 (brs, 1H,). ^{13}C NMR (62.5 MHz, $CDCl_3$): δ (ppm) 24.2, 71.5, 111.8, 119.0, 122.5, 62.5.4, 126.8, 129.0, 131.7, 132.4, 140.0, 148.8, 152.3, 171.2. Anal. Calcd for $C_{16}H_{13}N_3O$: C, 72.99; H, 4.98; N, 15.96 %; Found: C, 72.86; H, 4.86; N, 15.89 %.

5-Methyl-2-oxo-3-(phenylamino)indoline-3-carbonitrile (Compound 7ac)

White crystalline solid, mp: 109–111 °C (110–112) [65], υ_{max} (KBr): 3400, 3330, 3050, 2970, 2230, 1670 cm^{-1}. ^1H NMR (250 MHz, $CDCl_3$): δ (ppm) 2.20 (s, 3H), 5.05 (brs, 1H), 6.75 (s, 1H), 6.91–7.08 (brs, 2H), 7.99 (m, 5H), 9.95 (brs, 1H). ^{13}C NMR (62.5 MHz, $CDCl_3$): δ (ppm) 21.6, 71.5, 111.5, 119.0, 121.5, 62.5.4, 62.5.9, 126.0, 129.4, 131.8, 131.9, 132.9, 140.8, 171.0. Anal. Calcd for $C_{16}H_{13}N_3O$: C, 72.99; H, 4.98; N, 15.96 %; Found: C, 72.91; H, 4.95; N, 16.01 %.

3-(4-Bromophenylamino)-5-methyl-2-oxoindoline-3-carbonitrile (compound 7ad)

White crystalline solid, mp: 117–119 °C (119–121) [65], υ_{max} (KBr): 3410, 3300, 3030, 2980, 2220, 1670 cm^{-1}. ^1H NMR (250 MHz, $CDCl_3$): δ (ppm) 2.20 (s, 3H), 5.05 (brs, 1H), 6.74 (s, 1H), 6.99–7.08 (brs, 2H), 7.98–8.28 (m, 4H), 9.83 (brs, 1H). ^{13}C NMR (62.5 MHz, $CDCl_3$): δ (ppm) 22.5, 71.3, 111.8, 119.0, 122.0, 62.5.7, 62.5.8, 126.5, 129.3, 131.0, 131.9, 132.0, 140.5, 171.0. Anal. Calcd for $C_{16}H_{12}BrN_3O$: C, 56.16; H, 3.53; N, 12.28 %; Found: C, 56.02; H, 3.59; N, 12.39 %.

1,2-Dihydro-2-oxo-1-(phenylamino)acenaphthylene-1-carbonitrile (Compound 7ae)

Pale yellow crystalline solid, mp: 137–138 °C (135–137) [65], υ_{max} (KBr): 3465, 3050, 2980, 2220, 1695 cm^{-1}. ^1H NMR (250 MHz, $CDCl_3$): δ (ppm) 5.07 (brs, 1H), 7.44 (t, $J = 7.5$ Hz, 1H), 7.48–7.60 (m, 5H), 7.60 (d, $J = 7.5$ Hz, 1H), 7.82 (t, $J = 7.5$ Hz, 1H), 7.95 (d, $J = 7.5$ Hz, 1H), 7.99 (d, $J = 8.0$ Hz, 1H), 8.28 (d, $J = 8.0$ Hz, 1H). ^{13}C NMR (62.5 MHz, $CDCl_3$): δ (ppm) 73.0, 120.5, 121.1, 123.0, 126.2, 127.0, 128.5, 129.0, 129.4, 130.8, 131.1, 131.3, 132.5, 133.2, 134.6, 142.1, 196.2. Anal. Calcd for $C_{19}H_{12}N_2O$: C, 80.27; H, 4.25; N, 9.85 %; Found: C, 80.19; H, 4.20; N, 9.76 %.

1-(p-Tolylamino)-1,2-dihydro-2-oxoacenaphthylene-1-carbonitrile (Compound 7af)

Pale yellow crystalline, mp: 139–142 °C (138–140) [65], υ_{max} (KBr): 3490, 3030, 2960, 2220, 1695 cm^{-1}. ^1H NMR (250 MHz, $CDCl_3$): δ (ppm) 2.20 (s, 3H), 5.00 (brs, 1H), 7.40 (t, $J = 7.5$ Hz, 1H), 7.49–7.63 (m, 4H), 7.72 (d, $J = 7.5$ Hz, 1H), 7.79 (t, $J = 7.5$ Hz, 1H), 7.89 (d, $J = 7.5$ Hz, 1H), 8.01 (d, $J = 8.0$ Hz, 1H), 8.21 (d, $J = 8.0$ Hz, 1H). ^{13}C NMR (62.5 MHz, $CDCl_3$): δ (ppm) 22.6, 72.3, 120.5, 121.8, 123.6, 126.3, 127.0, 128.8, 129.0, 129.4, 130.2, 131.5, 131.6, 132.0, 133.2, 134.5, 142.4, 196.0. Anal. Calcd for $C_{20}H_{14}N_2O$: C, 80.52; H, 4.73; N, 9.39 %; Found: C, 80.48; H, 4.62; N, 9.47 %.

1-(4-Bromophenylamino)-1,2-dihydro-2-oxoacenaphthylene-1-carbonitrile Compound 7ag)

Pale yellow crystalline, mp: 170–173 °C (168–170) [65], υ_{max} (KBr): 3980, 3030, 2970, 2230, 1710 cm^{-1}. ^1H NMR (250 MHz, $CDCl_3$): δ (ppm) 5.15 (s, 1H), 7.40–7.49 (m, 2H,), 7.50–7.59 (m, 2H,), 7.66 (d, $J = 7.5$ Hz, 1H), 7.82 (d, $J = 8.5$ Hz, 1H), 7.89 (t, $J = 8.0$ Hz, 1H), 8.07 (d, $J = 8.5$ Hz, 1H), 8.19 (d, $J = 7.5$ Hz, 1H), 8.32 (d, $J = 8.5$ Hz, 1H). ^{13}C NMR (62.5 MHz, $CDCl_3$): δ (ppm) 71.6, 120.2, 121.3, 123.0, 127.4, 128.5, 129.0, 129.5, 130.3, 130.8, 131.5, 133.0, 134.5, 135.9, 142.8, 148.2, 196.0. Anal. Calcd for $C_{19}H_{11}BrN_2O$: C, 62.83; H, 3.05; N, 7.71 %; Found: C, 62.71; H, 3.01; N, 7.89 %.

2-(4-(3-(6-Amino-9H-purin-9-yl)propoxy)phenyl)-2-(phenylamino)acetonitrile (Compound 11)

White crystalline, mp: 234–237 °C. υ_{max} (KBr): 3370,2890, 2330, 1670, 1650, 1610, cm^{-1}. ^1H NMR (250 MHz, $CDCl_3$): δ (ppm) 2.07 (m, 2H), 3.63 (t, $J = 7.0$ Hz, 2H), 4.16 (t, $J = 7.0$ Hz, 2H), 5.31 (s, 1H), 6.23 (br, 2H), 6.39 (s, 1H), 6.86 (t, $J = 7.5$ Hz, 1H), 7.02- 7.13 (m, 6H), 7.59 (t, $J = 7.5$ Hz, 2H), 8.17 (s, 1H). ^{13}C NMR (62.5 MHz, $CDCl_3$): δ (ppm) 29.1, 41.7, 49.7, 69.1, 114.8, 116.2, 118.5, 119.3, 119.8, 128.6, 128.8, 130.3, 143.4, 145.7, 150.9, 152.3, 155.7, 157.9. Anal. Calcd for $C_{19}H_{11}BrN_2O$: C, 66.15; H, 5.30; N, 24.55 %; Found: C, 66.21; H, 5.38; N, 24.48 %. MS: m/z 399.18.

Results and discussions

In the first step, Fe_3O_4–BF_3 magnetic nanoparticles were prepared by stirring a mixture of Fe_3O_4 magnetic nanoparticles and $BF_3.Et_2O$ in toluene and calcination of obtained solid in 450 °C. The scanning electron microscopy (SEM) image of synthesized Fe_3O_4–BF_3 magnetic nanoparticles (Fig. 1) shows that the catalyst particles possess near-spherical morphology with relatively good monodispersity. In this study, the average diameter of magnetic nanoparticles was estimated to be $\sim$50 nm.

The XRD pattern of magnetic nanoparticles is shown in Fig. 2. Both Fe_3O_4 and Fe_3O_4–BF_3 magnetic nanoparticles show diffraction peaks at $2\theta = 30.3$, 35.6, 43.3, 53.8, 57.4 and 62.9 that are indexed to the crystalline cubic inverse spinel structure of Fe_3O_4 nanoparticles.

Figure 3 shows the infrared (IR) spectra of Fe_3O_4 magnetic nanoparticles and synthesized Fe_3O_4–BF_3 magnetic nanoparticles at different calcination temperatures over the 400–2000 cm^{-1} region. As shown in Fig. 3, all samples show characteristic peaks at 560 and 638 cm^{-1}, which are assigned to Fe–O stretching modes. The peak at 1083 is assigned to C–O (the residue of ether) that is not observed in the calcined samples. Apart from the main peaks of magnetic nanoparticles, there is a wide peak at $\sim$1400 cm^{-1}, which is assigned to B–O stretching.

Moreover the loading level of boron on the surface of F_3O_4 magnetic nanoparticles was estimated to be about 0.537 mmol g^{-1} as determined via the ICP method. To determine the bonding state of BF_3 and B/F mole ratios on the Fe_3O_4–BF_3 magnetic nanoparticles before and after heat treatment, the fluoride contents of freshly synthesized Fe_3O_4–BF_3 magnetic nanoparticles and calcinated Fe_3O_4–BF_3 magnetic nanoparticles at 450 °C were measured by a potentiometric method using a fluoride ion-selective electrode. Using this method, the B/F mole ratios for freshly synthesized Fe_3O_4–BF_3 magnetic nanoparticles and calcinated

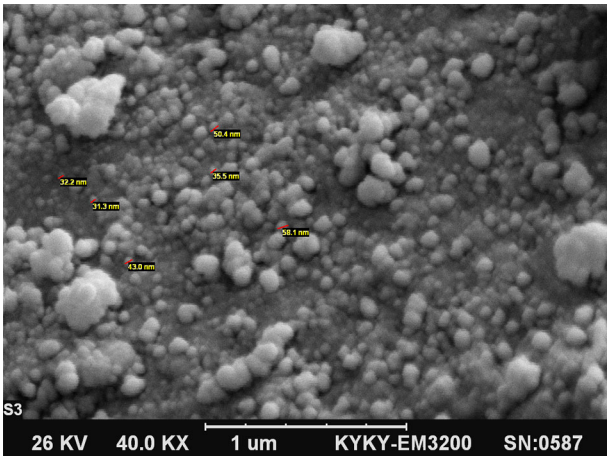

Fig. 1 The scanning electron microscopy (SEM) image of Fe_3O_4–BF_3 magnetic nanoparticles

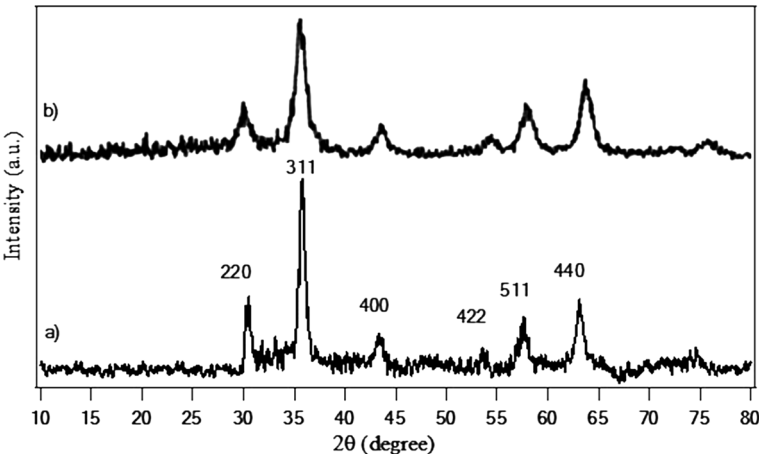

Fig. 2 The XRD pattern of Fe_3O_4 magnetic nanoparticles (*a*) and Fe_3O_4–BF_3 magnetic nanoparticles (*b*)

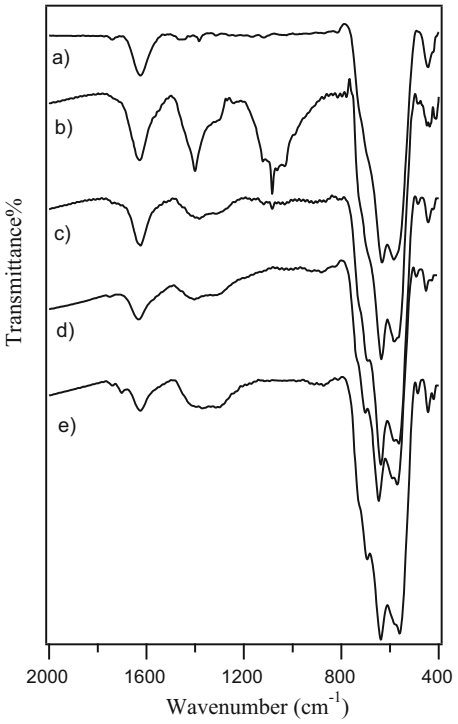

Fig. 3 FT-IR spectra of Fe_3O_4 magnetic nanoparticles (*a*), Fe_3O_4–BF_3 magnetic nanoparticles before calcination (*b*), Fe_3O_4–BF_3 magnetic nanoparticles after calcination at 350 °C (*c*), Fe_3O_4–BF_3 magnetic nanoparticles after calcination at 400 °C (*d*) and Fe_3O_4–BF_3 magnetic nanoparticles after calcination at 450 °C (*e*)

Fe_3O_4–BF_3 magnetic nanoparticles at 450 °C were obtained as 1/2.94 ≈ 1/3 and 1/1.93 ≈ 1/2, respectively. These results confirm the presence of BF_3 on the surface of freshly synthesized Fe_3O_4–BF_3 magnetic nanoparticles with bonding

interaction between the oxygen of Fe_3O_4 magnetic nanoparticles and the boron of BF_3. The B/F mole ratio of 1/2 in calcinated Fe_3O_4–BF_3 magnetic nanoparticles also confirms the presence of a covalent bond between the oxygen of Fe–O and boron and formation of –O–BF_2 due to evolution of hydrofluoric acid (HF) during the calcination. Thus, Fe–O–BF_2 is the final structural form of the catalyst in calcinated Fe_3O_4–BF_3 magnetic nanoparticles.

The catalyst acidity characters, including the acidic strength and the total number of acid sites were determined by a potentiometric titration. According to this method, the initial electrode potential (E_i) indicates the maximum acid strength of the surface sites and the range of where a plateau is reached (mili-equivalents of used *n*-butylamine per gram of the catalyst) indicates the total number of acid sites [64]. Therefore, a suspension of the catalyst in acetonitrile was potentiometrically titrated with a solution of 0.02-molar *n*-butylamine and obtained results are summarized in Fig. 4. As shown in Fig. 4, Fe_3O_4–BF_3 magnetic nanoparticles display higher strength than the Fe_3O_4 magnetic nanoparticles.

Moreover, magnetization properties of Fe_3O_4 magnetic nanoparticles and Fe_3O_4–BF_3 magnetic nanoparticles were investigated using the vibrating sample magnometer (VSM) and obtained results are shown in Fig. 5. Based on these results, the saturation magnetization value was measured to be 60 emu g^{-1} for Fe_3O_4 magnetic nanoparticles and 50 emu g^{-1} for Fe_3O_4–BF_3 magnetic nanoparticles. The results show that in this case, surface modification has an insignificant effect on the magnetic properties of Fe_3O_4 magnetic nanoparticles.

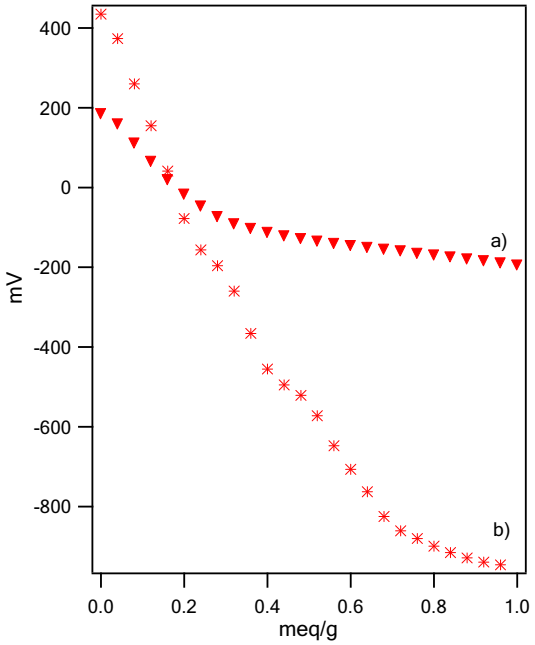

Fig. 4 Potentiometric titration of (*a*) Fe_3O_4 magnetic nanoparticles and (*b*) Fe_3O_4–BF_3 magnetic nanoparticles

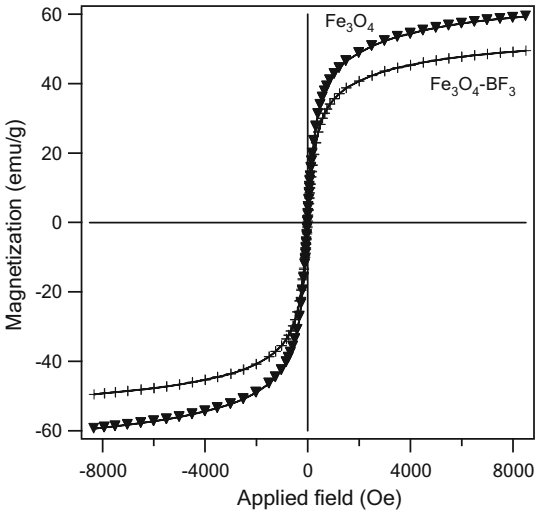

Fig. 5 The magnetisation behaviour of Fe_3O_4 magnetic nanoparticles and Fe_3O_4–BF_3 magnetic nanoparticles

In the next step, to introduce the applicability of Fe_3O_4–BF_3 magnetic nanoparticles as a new magnetically separable Lewis acid, its efficiency was explored in a three-component reaction of carbonyl compounds with amines and TMSCN under ultrasonic irradiation (Scheme 1).

To find an appropriate reaction medium for the synthesis of titled compounds in the presence of Fe_3O_4–BF_3 magnetic nanoparticles, the one-pot three-component condensation of benzaldehyde (1 mmol), aniline (1.2 mmol) and trimethylsilyl cyanide (1.2 mmol) was selected as a model reaction and was examined in several reaction mediums; the yield and reaction times were monitored in the presence of ultrasonic irradiation at room temperature and obtained results are summarized in Table 1.

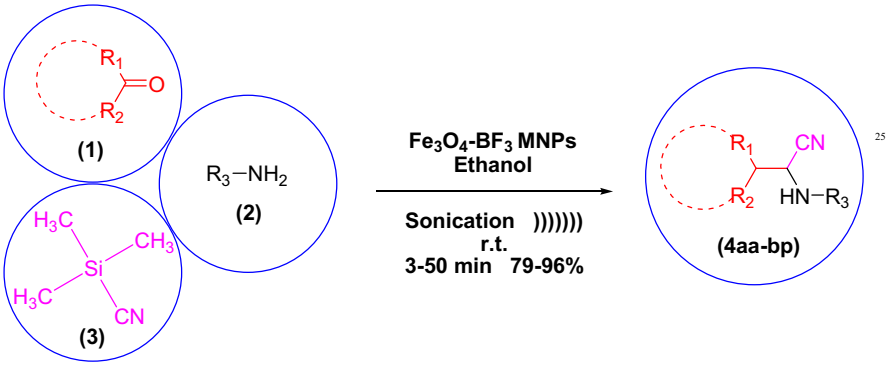

Scheme 1 The ultrasound-promoted one-pot three-component synthesis of α-aminonitriles using Fe_3O_4–BF_3 magnetic nanoparticles as a new magnetically separable Lewis acid catalyst

As it is clear from Table 1, the best results were obtained in the presence of only 50 milligrams of Fe_3O_4–BF_3 magnetic nanoparticles in ethanol as a solvent (Table 1, entry 6). However, the increasing amount of Fe_3O_4–BF_3 magnetic nanoparticles does not affect the reaction yield and time (Table 1, entry 8), but the reaction yield was decreased in the presence of lower amount of Fe_3O_4–BF_3 magnetic nanoparticles (Table 2, entry 7). Moreover, the model reaction was investigated in the absence of a catalyst and the reaction did not proceed even after a long time of ultrasonic irradiation (Table 1, entry 9). In another study, the model reaction was investigated in the presence of Fe_3O_4 magnetic nanoparticles (50 mg) and the reaction did not proceed even after a long time of ultrasonic irradiation. These observations establish the crucial role of Fe_3O_4–BF_3 magnetic nanoparticles as a Lewis acid catalyst.

More recently, we introduced sulfuric acid-modified PEG-6000 (PEG-OSO_3H) as an efficient Brönsted acid-surfactant combined catalyst for the synthesis of α-aminonitriles and very good results were obtained [62]. So, in order to examine the scope and efficiency of Fe_3O_4–BF_3 magnetic nanoparticles as a new heterogeneous magnetically separable Lewis acid catalyst, production of all previously synthesized α-aminonitriles (that were synthesized in the presence of PEG-SO_3H) was explored under the optimized conditions. For this purpose, a broad range of structurally diverse aldehydes (aliphatic and aromatic) as well as ketones and amines (aliphatic or aromatic) were condensed with trimethylsilyl cyanide and results are displayed in Table 2. As can be seen from Table 2, all reactions proceeded efficiently and desired products were obtained in good to excellent yields in relatively short reaction times without formation of any byproducts. Aromatic aldehydes having electron-withdrawing groups (Table 2, entries 4an, 4ao and 4at) reacted at faster rates compared with those that substituted with electron-releasing groups (Table 2, entries 4aq, 4ar and 4as). Besides, the presented method has been successfully used for heteroaromatic aldehydes as acid- and base-sensitive compounds and corresponding α-aminonitriles were obtained in excellent yields without any byproducts (Table 2, entries 4au, 4av

Table 1 The three-component reaction between benzaldehyde (1 mmol), aniline (1.2 mmol) and trimethylsilyl cyanide (1.2 mmol) in several reaction mediums under ultrasonic irradiation at room temperature in the presence of Fe_3O_4–BF_3 magnetic nanoparticles

Entry	Solvent (5 mL)	Catalyst (mg)	Time (min)	Yield (%)[a]
1	Dichloromethane	50	60	Trace
2	Chloroform	50	60	25
3	Ethyl acetate	50	60	49
4	Methanol	50	10	93
5	Water	50	35	81
6	Ethanol	50	5	94
7	Ethanol	40	20	87
8	Ethanol	70	5	94
9	Ethanol	–	60	No reaction

[a] Isolated yield

Table 2 Ultrasound-assisted synthesis of α-aminonitriles using Fe_3O_4–BF_3

Entry	R^1	R^2	Time (min)	Yield (%)[a]
4aa	C_6H_5	C_6H_5	5	90
4ab	C_6H_5	3,4-CH_3-C_6H_3	7	90
4ac	C_6H_5	4-Br-C_6H_4	5	89
4ad	C_6H_5	4-CH_3-C_6H_4	5	90
4ae	C_6H_5	–$CH_2CH_2OCH_2CH_2$–	25	87
4af	C_6H_5	C_6H_5-CH_2	30	88
4ag	C_6H_5	$CH_3CH_2CH_2CH_2$	35	85
4ah	C_6H_5	$(CH_3)_2CH$	30	85
4ai	C_6H_5	–$CH_2CH_2CH_2CH_2$–	30	88
4aj	C_6H_5	4-Cl-C_6H_4	8	90
4ak	C_6H_5	1-Naphthyl	25	84
4al	4-Cl-C_6H_4	4-CH_3-C_6H_4	5	91
4am	4-Cl-C_6H_4	C_6H_5	5	90
4an	4-F-C_6H_4	C_6H_5	6	89
4ao	4-F-C_6H_4	4-CH_3-C_6H_4	6	90
4ap	2,4-Cl-C_6H_3	4-CH_3-C_6H_4	20	88
4aq	4-OCH_3-C_6H_4	C_6H_5	25	85
4ar	3-OCH_3-C_6H_4	$CH_3CH_2CH_2CH_2$	30	81
4as	3-OCH_3-C_6H_4	C_6H_5	30	86
4at	3-NO_2-C_6H_4	C_6H_5	3	92
4au	2-Thienyl	C_6H_5-CH_2	15	91
4av	2-Furyl	C_6H_5-CH_2	15	89
4aw	3-Pyridyl	$CH_3CH_2CH_2CH_2$	35	81
4ax	4-CH_3-C_6H_4	C_6H_5	15	89
4ay	1-Naphthyl	C_6H_5	25	83
4az	$CH_3CH_2CH_2CH_2$	C_6H_5	20	81
4ba	$(CH_3)_2CH$	C_6H_5-CH_2	25	81
4bb	$(CH_3)_2CH$	–$CH_2CH_2CH_2CH_2$–	30	79

Reaction condition: aldehyde or ketone (1 mmol), amine (1.2 mmol), trimethylsilyl cyanide (1.2 mmol), ethanol (5 mL) and Fe_3O_4–BF_3 (5 mg), ultrasonic irradiation (40 kHz, 200 W) at room temperature

[a] Yields refer to isolated pure products

and 4aw). As it is clear from the obtained results, the presented methodology can be used in order of oxygen-, sulfur- and nitrogen-containing heteroaromatic aldehydes. Interestingly, cyclic ketones such as cyclopentanone, cyclohexanone and cycloheptanone, as well as aryl–alkyl ketones, diaryl ketones and tetralones, were successfully reacted with amines and trimethylsilyl cyanide to afford corresponding α-aminonitriles in reasonable yields and in short reaction times (Table 2, entries 4bc-bm and 4 bp). In the case of aliphatic amines, relatively slow reaction rates occurred due to the

unstable nature of formed aliphatic imines in the presence of water (Table 2, entries 4ae, 4af, 4aq, 4ah, 4ai, 4ar, 4au, 4av and 4aw).

Oxindole derivatives exhibit an extensive range of biological effects. For example, indolin-2-one (Sunitinib) has been widely used in the treatment of gastrointestinal stromal tumors, and metastatic renal cell cancer. Oxindole-Schiff base copper (II) complexes have shown potential antitumor activity towards different cells. Moreover, indolidan and adibendan are used for the treatment of congestive heart failure as these have strong vasodilatory, positive inotropic and inodilatory actions. Amino methylene oxindole derivatives are useful as antihypertensive agents and oxindole-oxazolidinone derivatives are the most important class of antimicrobial compounds. Artificial oxindole-containing compounds also exhibit useful pharmaceutical properties, including growth hormone secretagogues, analgesic, anti-inflammatory, and serotonergic. Most of these compounds contain a variety of substituent at the C-3 position of oxindole [66–78]. Considering these facts, new α-aminonitriles bearing an indoline moiety were synthesized via a one-pot three-component condensation reaction between isatin derivatives (**5**), amines and trimethylsilyl cyanide in the presence of Fe_3O_4–BF_3 magnetic nanoparticles under ultrasonic irradiation at room temperature. Moreover, acenaphthenequinone (**6**) was applied successfully for the first time and desired α-aminonitriles were obtained in excellent yields and relatively short reaction times; obtained results are summarized in Table 3 (Scheme 2).

Adenine is a nucleobase with a variety of roles in biochemistry, including cellular respiration and protein synthesis as a chemical component of DNA and RNA. Moreover, it is the certain backbone of various commercial antivirus drugs such as Adefovir, Tenofovir and Adefovir dipivoxil. In addition, various α-aminonitrile compounds have been reported for their biological as well as pharmaceutical properties such as reversible inhibition of dipeptidyl peptidase-4 (DPP-4) for the treatment of diabetes. As a stimulant drug, amphetaminil has been used for the treatment of obesity and narcolepsy. Saxagliptin is a new anti-diabetic drug that is classified as a potent dipeptidyl peptidase-4 (DPP-4) inhibitor agent. Another most important dipeptidyl peptidase-4 (DPP-4 inhibitor) is vildagliptin, which has been used as an efficient anti-diabetic drug in recent years. Based on these facts, combination of amionitrile moiety with an adenine backbone may be lead to the construction of new biological active compounds with unique and special properties. With this point of view, we examined our method for the synthesis of a new adenine-containing α-aminonitrile. For this, compound (**1b**) was synthesized in two steps. At first, 4-hydroxybenzaldehyde (**1c**) was reacted with 1,3-dibromopropane (**8**) to produce 4-(3-bromopropoxy)benzaldehyde (**9**). Finally, presilylated adenine (**10**) was added to compound (**9**) and aldehyde (**1b**) was obtained in good yield (Scheme 3).

To assess the capability and efficiency of our methodology with respect to the reported procedures for the synthesis of α-aminonitriles, results of the application of these methods are tabulated in Table 4. As it is clear from Table 4, our presented methodology was more efficient.

The possibility of recycling the catalyst was examined using the one-pot three-component reaction between benzaldehyde (1 mmol), aniline (1.2 mmol) and

Table 3 The condensation reaction of isatins (**5**) as well as acenaphthenequinone (**6**) with amines and TMSCN in the presence of magnetic Fe_3O_4–BF_3 under ultrasonic irradiation at room temperature

Entry	Carbonyl compound	Amine	Product	Time (min)	Yield (%)[a]	M.P. (°C)
7aa			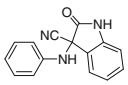	8	89	93–94 (91–92 [65])
7ab		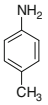	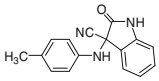	6	92	101–103 (99–101 [65])
7ac	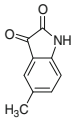		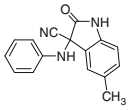	8	90	109–111 (110–112 [65])
7ad	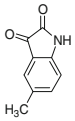	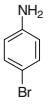	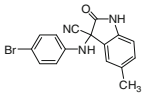	8	94	118–120 (119–121 [65])
7ae			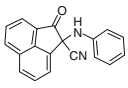	10	94	133–135 (135–137 [65])
7af		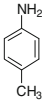	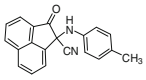	8	91	134–136 (138–140 [65])
7ag		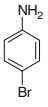	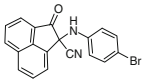	10	93	167–169 (168–170 [65])

[a] Isolated yields

trimethylsilyl cyanide (1.2 mmol) under the optimized conditions. After completion of the reaction, catalyst was removed with a magnet washed with ethanol, dried and reused. After the isolation of catalyst, water (20 mL) was added and insoluble crude products were filtered and recrystallized from ethanol/water (4:1). In the case of oil products, appropriate amounts of ethyl acetate (5 mL, two times) were added, the organic layer was washed with brine (5 mL), dried ($MgSO_4$), and concentrated. The residue was chromatographed over silica gel (15-% ethyl acetate in *n*-hexane) to give a pure product. Recovered Fe_3O_4–BF_3 magnetic nanoparticles were reused 15 times in the condensation of benzaldehyde (1 mmol), aniline (1.2 mmol) and trimethylsilyl cyanide (1.2 mmol) and any loss of efficiency was not observed (Fig. 6). In order to study the stability of the catalyst structure, the boron content of the catalyst was determined to be at about 0.5 mmol g^{-1} after the 15th reuse. So, it has been concluded that the catalyst structure is stable under the reaction condition and boron is strongly bonded to the surface of Fe_3O_4 magnetic nanoparticles and was not leached during the reaction.

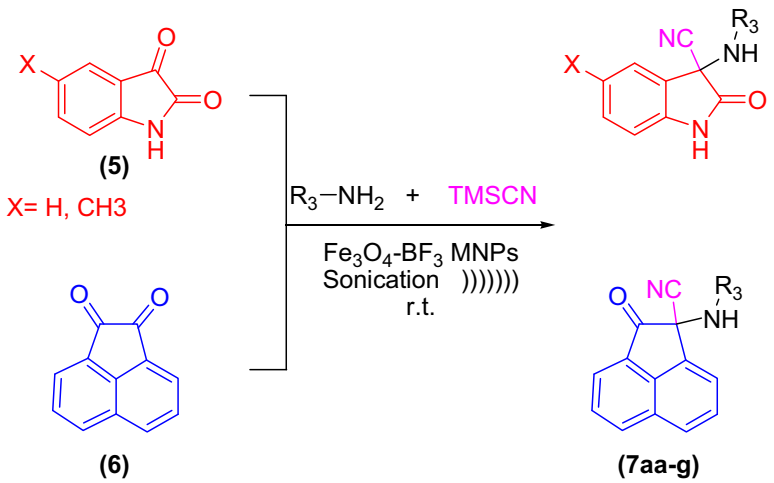

Scheme 2 Ultrasound-assisted one-pot three-component condensation of isatin derivatives (**5**) and acenaphthenequinone (**6**) with amines and trimethylsilyl cyanide in the presence of Fe_3O_4–BF_3 at room temperature

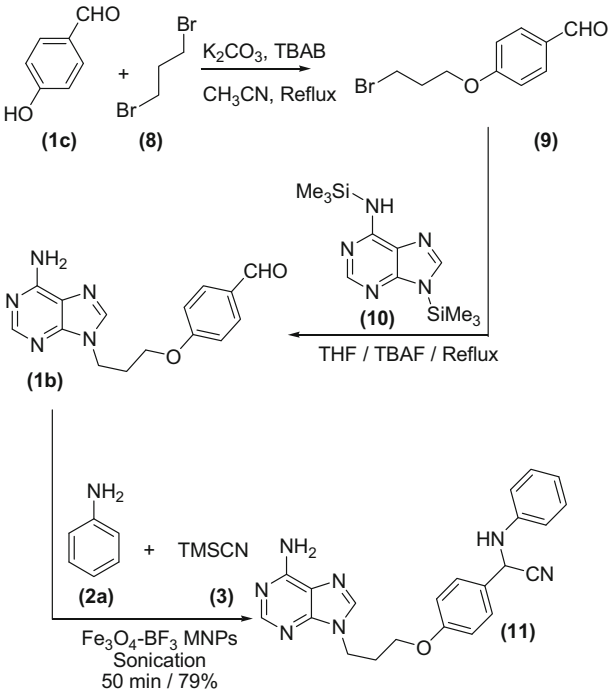

Scheme 3 Synthesis of an adenine-containing starting material for the synthesis of an adenine-containing α-aminonitrile (**11**)

Table 4 Comparison of the condensation of benzaldehyde and aniline with trimethylsilyl cyanide using the reported methods versus the present method

Entry	Conditions	Time (min)	Yield (%)	Refs.
1	$InCl_3$ (20 mol%), Dry tetrahydrofurane, room temperature	360	75	[19]
2	$BiCl_3$ (10 mol%), acetonitrile, room temperature	600	84	[20]
3	Montmorillonite KSF clay, 1.0 g, dichloromethane, room temperature	210	90	[21]
4	Silica-based scandium(III) (3 mol%), dichloromethane, room temperature	840	94	[22]
5	SO_4^{2-}/ZrO_2 (10 mol%), Dry tetrahydrofurane, N_2 atmosphere, room temperature	90	93	[23]
6	Guanidine hydrochloride (3 mol%), ethanol, 40 °C	60	94	[31]
7	Xanthane sulfuric acid (6 mol%), Dry acetonitrile, room temperature	65	97	[32]
8	Silica sulfuric acid (25 mol%), dichloromethane, room temperature	360	88	[34]
9	SBA-15 supported sulfonic acid (5 mol%), solvent-free 50 °C	5	100	[35]
10	Fe_3O_4–BF_3 magnetic nanoparticles (50 mg), ethanol, ultrasonic irradiation, room temperature	5	94	This work

A plausible mechanism for the preparation of titled compounds in the presence of Fe_3O_4–BF_3 as a magnetically separable Lewis acid catalyst is described in Scheme 4. As it is shown in Scheme 4, at first, desired imines (**12**) will be produced with the condensation of carbonyl compounds (**1**) and amines (**2**). In the next step, prepared imines will be attacked with the cyanide ion that is released from the trimethylsilyl cyanide (**3**) in the presence of water to produce the desired α-aminonitriles. The crucial role of Fe_3O_4–BF_3 as a magnetically separable Lewis acid catalyst is to increase the electrophilicity of carbonyl compounds toward the nucleophilic attack of amines with the interaction of borane and oxygen of carbonyl compounds. Moreover, readily formed imines will be activated toward the nucleophilic attack of cyanide ions with the interaction of borane and the nitrogen of imines.

Moreover the energy-based efficiency (η_e) of the reaction was calculated for the model reaction. Based on the assumption that the mechanical energy generated by the ultrasonic waves is reduced to heat, the dissipated ultrasonic power U_p was calculated from the rate of temperature increase as:

$$U_p = C_p M \cdot \frac{dT}{dt}$$

where C_p is the heat capacity of the solvent at constant pressure (J g^{-1} K^{-1}), M is the mass of solvent (g) and dT/dt is temperature rise per second [79]. The dT/dt was determined to be at about 1 K s^{-1} under the applied conditions. So, based on this equation and for ethanol as solvent ($C_p = 2.44$ J g^{-1} K^{-1}, 3.945 g) and 5 min

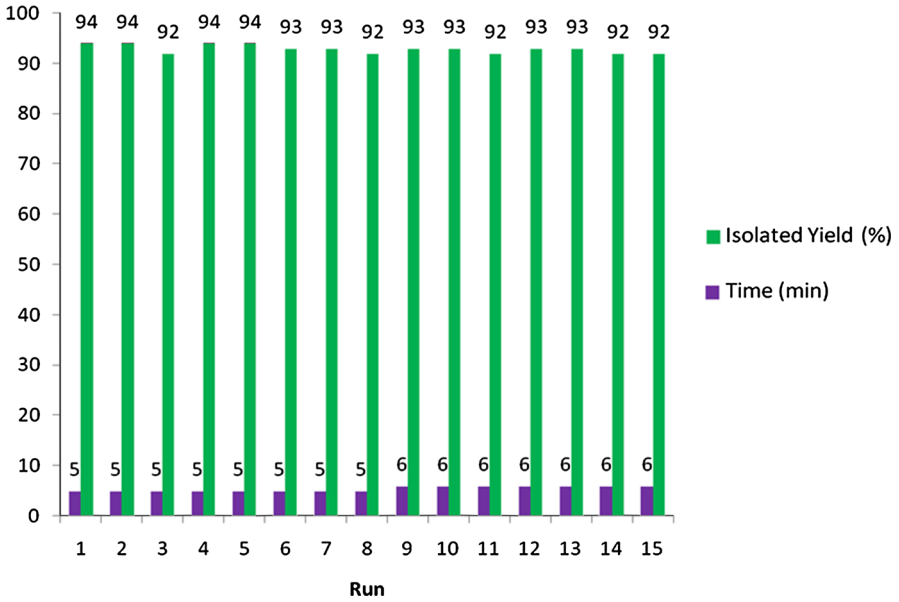

Fig. 6 The reusability and recyclability of magnetic Fe_3O_4–BF_3 catalyst

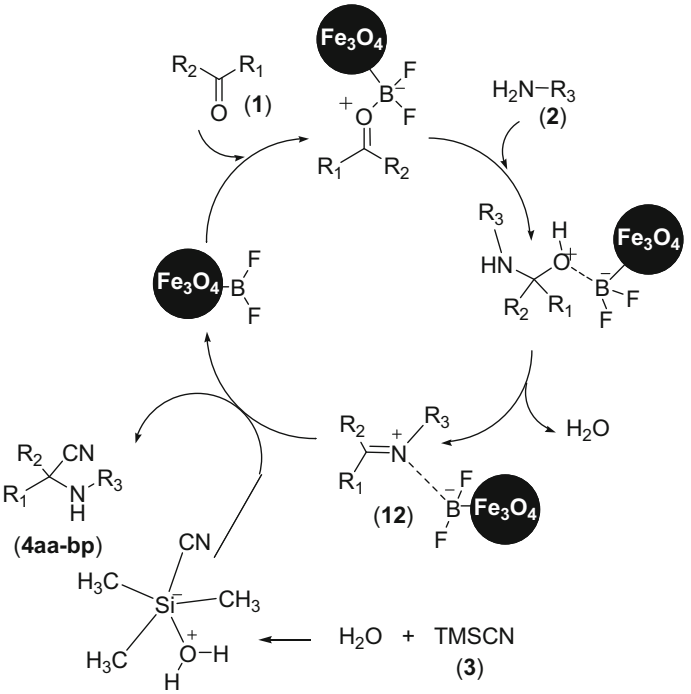

Scheme 4 The plausible mechanism for the synthesis of α-aminonitriles in the presence of Fe_3O_4–BF_3

irradiation (300 s), the U_p was calculated to be at around 2887.74 Jules. The electrical power supply of the ultrasound generator worked with 280-W power and the power of produced ultrasonic irradiation was calculated to be 200 W. The energy-based efficiency was calculated as follows, where P_u is the ultrasonic power and P_e is the electrical power:

$$\eta_e = \frac{P_u - U_p}{P_e}$$

Using this equation and for applied conditions (5 min ultrasonic irradiation, 5-mL ethanol as solvent), the energy-based efficiency of the applied method for the model reaction was calculated to be 0.67.

Conclusions

In summary, we have reported a new, highly efficient and sustainable catalytic system for the synthesis of α-aminonitriles. In this context, covalence bonding of BF_3 as a strong Lewis acid on the surface of Fe_3O_4 magnetic nanoparticles changes this material from a very hazardous and non-recyclable chemical to a heterogeneous magnetically separable solid Lewis acid. Application of this catalyst not only offers substantial improvements in the reaction rates and yields, but also avoids the use of hazardous catalysts or solvents. The promising points for the presented methodology are efficiency, generality, high yields, short reaction times, cleaner reaction profiles, ease of product isolation, simplicity and, finally, agreement with the green chemistry protocols which all make it a useful and attractive process for the synthesis of α-aminonitriles.

Acknowledgments We gratefully appreciate the Shiraz University Research Council for their financial support of this work.

References

1. J. Grunes, J. Zhu, G.A. Somorjai, Chem. Commun. **18**, 2257 (2003)
2. A.T. Bell, Science **299**, 1688 (2003)
3. R. Schlgl, S.B. Abd Hamid, Angew. Chem. **116**, 1656 (2004)
4. R. Schlgl, S.B. Abd Hamid, Angew. Chem. Int. Ed. **43**, 1628 (2004)
5. W. Teunissen, A.A. Bol, J.W. Geus, Catal. Today **48**, 329 (1999)
6. J.M. Campelo, D. Luna, R. Luque, J.M. Marinas, A.A. Romero, ChemSusChem **2**, 18 (2009)
7. G. Glaspell, H.M.A. Hassan, A. Elzatahry, V. Abdalsayed, M.S. El-Shall, Top. Catal. **47**, 22 (2008)
8. P. Claus, A. Bruckner, C. Mohr, H. Hofmeister, J. Am. Chem. Soc. **122**, 11430 (2000)
9. A. Martino, S.A. Yamanaka, J.S. Kawola, D.A. Ly, Chem. Mater. **9**, 423 (1997)
10. X.D. Mu, D.G. Evans, Y. Kou, Catal. Lett. **97**, 151 (2004)
11. C.B. Hwang, Y.S. Fu, Y.-L. Lu, S.-W. Jang, P.-T. Chou, C.-R. Wang, S.-J. Yu, J. Catal. **195**, 336 (2000)
12. J.A. Dahl, B.L.S. Maddux, J.E. Hutchinson, Chem. Rev. **107**, 2228 (2007)
13. R. Narayanan, M.A. El-Sayed, J. Phys. Chem. B **109**, 12663 (2005)
14. R.B.N. Baig, M.N. Nadagouda, R.S. Varma, Green Chem. **16**, 4333 (2014)
15. S. Verma, S.L. Jain, B. Sain, ChemCatChem **3**, 1329 (2011)
16. R.B.N. Baiga, R.S. Varma, Chem. Commun. **49**, 752 (2013)

17. R.B.N. Baig, M.N. Nadagouda, R.S. Varma, Coord. Chem. Rev. **287**, 137 (2015)
18. D. Verma, S. Verma, A.K. Sinha, S.L. Jain, ChemPlusChem **78**, 860 (2013)
19. L. Deloux, M. Srebnik, Chem. Rev. **93**, 763 (1993)
20. H. Heaney, Boron trifluoride, in *Encyclopedia of Reagents for Organic Synthesis*. ISBN 0-471-93623-5 (2001). doi:10.1002/047084289X.rb250
21. A. Strecker, Ann. Chem. Pharm. **75**, 27 (1850)
22. Y.M. Shafran, V.S. Bakulev, V.S. Mokrushin, Russ. Chem. Rev. **58**, 148 (1989)
23. J. March, *Advanced Organic Chemistry*, 4th edn. (Wiley, New York, 1995), p. 965
24. L.M. Weinstock, P. Davis, B. Handelsman, R. Tull, J. Org. Chem. **32**, 2823 (1967)
25. W.L. Matier, D.A. Owens, W.T. Comer, D. Dietchman, H.C. Ferguson, R.J. Seidehamel, J.R. Young, J. Med. Chem. **16**, 901 (1973)
26. R.O. Duthaler, Tetrahedron **50**, 1539 (1994)
27. H. Groger, Chem. Rev. **103**, 2795 (2003)
28. S. Kobayashi, H. Ishitani, Chem. Rev. **99**, 1069 (1999)
29. S. Harusawa, Y. Hamada, T. Shioiri, Tetrahedron Lett. **20**, 4663 (1979)
30. P. Vachal, E.N. Jacobsen, J. Am. Chem. Soc. **124**, 10012 (2002)
31. S. Nakamura, N. Sato, M. Sugimoto, T. Toru, Tetrahedron Asymmetry **15**, 1513 (2004)
32. B.C. Ranu, S.S. Dey, S. Hajra, Tetrahedron **58**, 2529 (2002)
33. S.K. De, R.A. Gibbs, Tetrahedron Lett. **45**, 7407 (2004)
34. J.S. Yadav, B.V.S. Reddy, B. Eswaraiah, M. Srinivas, Tetrahedron **60**, 1767 (2004)
35. B. Karimi, A.A. Safari, J. Organomet. Chem. **693**, 2967 (2008)
36. B.M. Reddy, B. Thirupathi, M.K. Patil, J. Mol. Catal. A: Chem. **307**, 154 (2009)
37. H.A. Oskooie, M.M. Heravi, A. Sadnia, F. Jannati, F.K. Behbahani, Synth. Commun. **37**, 2543 (2007)
38. N.H. Khan, S. Agrawal, R.I. Kureshy, S.H.R. Abdi, S. Singh, E. Suresh, R.V. Jasra, Tetrahedron Lett. **49**, 640 (2008)
39. Z.L. Shen, S.J. Ji, T.P. Loh, Tetrahedron **64**, 8159 (2008)
40. S.H. Wang, L.F. Zhao, Z.M. Du, Chin. J. Chem. **24**, 135 (2006)
41. E. Rafiee, A. Azad, Synth. Commun. **37**, 1127 (2007)
42. S.K. De, Synth. Commun. **35**, 1577 (2005)
43. M.M. Mojtahedi, S. Abaee, T. Alishiri, Tetrahedron Lett. **50**, 2322 (2009)
44. A. Heydari, A. Arefi, S. Khaksar, R.K. Shiroodi, J. Mol. Catal. A: Chem. **271**, 142 (2007)
45. A. Shaabani, A. Maleki, M.R. Soudi, H. Mofakham, Catal. Commun. **10**, 945 (2009)
46. J.S. Yadav, B.V.S. Reddy, B. Eshwaraiah, M. Srinivas, P. Vishnumurthy, New J. Chem. **27**, 462 (2003)
47. W.Y. Chen, J. Lu, Synlett 2293 **15**, (2005)
48. B. Karimi, D. Zareyee, J. Mater. Chem. **19**, 8665 (2009)
49. K. Niknam, D. Saberi, M. Nouri Sefat, Tetrahedron Lett. **51**, 2959 (2010)
50. B.A. Bhanu, A. Bisai, V.K. Singh, Tetrahedron Lett. **45**, 9565 (2004)
51. J.S. Yadav, B.V. Subba Reddy, B. Eeshwaraiah, M. Srinivas, Tetrahedron **60**, 1767 (2004)
52. A. Heydari, P. Fatemi, A.A. Alizadeh, Tetrahedron Lett. **39**, 3049 (1998)
53. J. Lablanc, H.W. Gibson, Tetrahedron Lett. **33**, 6295 (1992)
54. T.K. Chakraborty, G.V. Reddy, K.A. Hussain, Tetrahedron Lett. **32**, 7597 (1991)
55. H.A. Oskooie, M.M. Heravi, K. Bakhtiari, V. Zadsirjan, F.F. Bamoharram, Synlett **11**, 1768 (2006)
56. A. Baeza, C. Nájera, J.M. Sansano, Synthesis **8**, 1230 (2007)
57. I.V.P. Raj, G. Suryavanshi, A. Sudalai, Tetrahedron Lett. **48**, 7211 (2007)
58. A. Khalafi-Nezhad, S. Mohammadi, RSC Adv. **4**, 13782 (2014)
59. A. Khalafi-Nezhad, M. Divar, F. Panahi, RSC Adv. **5**, 2223 (2015)
60. A. Khalafi-Nezhad, M. Nourisefat, F. Panahi, RSC Adv. **4**, 22497 (2014)
61. R. Ghosh, L. Pradhan, Y.P. Devi, S.S. Meena, R. Tewari, A. Kumar, S. Sharma, N.S. Gajbhiye, R.K. Vatsa, B.N. Pandey, R.S. Ningthoujam, J. Mater. Chem. **21**, 13388 (2011)
62. W. Frenzel, P. Brätter, Anal. Chim. Acta **188**, 151 (1986)
63. M.N. Soltani Rad, A. Khalafi-Nezhad, M. Divar, S. Behrouz, Phosphorus Sulfur Silicon **185**, 1943 (2010)
64. L.R. Pizzio, P.G. Vázquez, C.V. Cáceres, M.N. Blanco, Appl. Catal. A Gen. **256**, 125 (2003)
65. M. Shekouhy, Catal. Sci. Technol. **2**, 1010 (2012)
66. S.R.S. Rudrangi, V.K. Bontha, V.R. Manda, S. Bethi, Asian J. Res. Chem **4**, 335 (2011)
67. B.V. Silva, N.M. Ribeiro, A.C. Pinto, M.D. Vargas, L.C.J. Dias, Braz. Chem. Soc. **19**, 1244 (2008)
68. S.B. Kadin, *Google Patents*, EP0244918 B1 (1985)

69. J.J. Kyncl, M. Winn, *Google Patents*, US4176191 A(1979)
70. G.E. Hardtmann, *Google Patents*, US4160032 A (1979)
71. V.P. Josyula, G. Luehr, M. Gordeev, *Google Patents*, US20060229349 A1 (2006)
72. N.T. Zaveri, F. Jiang, C.M. Olsen, J.R. Deschamps, D. Parrish, W. Polgar, L. Toll, J. Med. Chem. **47**, 2973 (2004)
73. M. Alcaraz, S. Atkinson, P. Cornwall, A.C. Foster, D.M. Gill, L.A. Humphries, P.S. Keegan, R. Kemp, E. Merifield, R.A. Nixon, A.J. Noble, D. O'Beirne, Z.M. Patel, J. Perkins, P. Rowa, P. Sadler, J.T. Singleton, J. Tornos, A.J. Watts, I.A. Woodland, Org. Process Res. Dev. **9**, 555 (2005)
74. C. Kikuchi, T. Hiranuma, M. Koyama, Bioorg. Med. Chem. Lett. **12**, 2549 (2002)
75. R. Gallagher Jr., G.L. Patricia, W.W. James, J.P. Hieble, R.M. DeMarinis, J. Med. Chem. **28**, 1533 (1985)
76. Y. Koguchi, J. Kohno, M. Nishio, K. Takahashi, T. Okuda, T. Ohnuki, S.J. Komatsubara, Antibiotics **53**, 105 (2000)
77. C.D. Smith, J.T. Zilfou, K. Stratmann, G.M.L. Patterson, R.E. Moore, Mol. Pharmacol. **47**, 241–247 (1995)
78. H. Pajouhesh, R. Parson, F.D. Popp, J. Pharm. Sci. **72**, 318 (1983)
79. T.J. Mason, J.P. Lorimer, D.M. Bates, Ultrasonics **30**, 40 (1992)